INFRARED PHOTOMETRY OF THE 1982-4 ECLIPSE OF EPSILON AURIGAE

D. E. Backman

Institute for Astronomy
University of Hawaii

The infrared photometry of ϵ Aur performed prior to and during the ingress phase of the recent eclipse allowed the first solid determination of the temperature of the secondary object. The eclipse depth was significantly less at $\lambda > 5$ μm than in the near-infrared. This is explained by a model of the secondary as an opaque and very cool object with a temperature of ~500 K.

During eclipse, the secondary blocks approximately 47% of the near-infrared radiation from the primary star. At the same time, the radiation from the secondary remains completely unobscured, resulting in a shallower light curve at longer wavelengths. This phenomenon is well known in the study of eclipsing binary stars; if the two stars have different colors, then the net color of the system changes during eclipse. In the case of ϵ Aur, the eclipsing object has a "color" deep in the infrared, so the effect is only noticeable there.

The infrared measurements were made by a group of collaborators at the University of Hawaii and Kitt Peak National Observatory of the National Optical Astronomy Observatories†† Figure 1 is a comparison of the shapes of the visual and infrared light curves at three wavelengths during the fall 1982 eclipse ingress. The K band (2.2 μm) is plotted as representative of the entire near infrared; the light curves in the five near infrared bands (J, H, K, L, and M) were identical to within the observational errors. The depth of the infrared eclipse is referred to our pre-eclipse measurements, which were made from 2-1/2 years up until 4 months prior to the predicted date of first contact. The visual points plotted are measurements made by Dietmar Böhme in East Germany, which we received before Hopkins' first compendium (Hopkins and Stencel 1983). We are unable to make a direct comparison between the visual and infrared eclipse depths with the data shown in this figure because Böhme had no pre-eclipse data from dates as far prior to eclipse as ours. The well-known small amplitude pulsations of the primary are one of the reasons why the pre-eclipse baseline magnitudes depend on the epoch of observation; another would be the presence of any gentle "roll-on" of the eclipse in the months prior to first contact. We normalized Böhme's data to ours in this plot using the post-second contact mean magnitudes.

Strictly speaking, our UH/KPNO results come from a comparison of the infrared light curves at $\lambda \leq 5$ μm and $\lambda > 5$ μm. We can only indirectly conclude in addition that the visual and the near-infrared behaviors are identical, by pointing out that the ingress slopes at 2.2 μm and in the visual are the same and that our near-infrared depth for this ingress was similar to the visual depth in the 1955-7 eclipse.

On the basis of our infrared results, we concluded (Backman *et al.* 1984) that the secondary object has a temperature of 500 K. We used two ways to evaluate the amount of infrared radiation coming from the secondary object and thereby determine its temperature. The first method made use only of the dependence of eclipse depth on

††Operated by the Association of Universities for Research in Astronomy, Inc. under contract with the National Science Foundation.

wavelength in order to separate the relative flux contributions at each wavelength from the primary and the secondary. The second method involved extrapolating the primary star's spectrum from the near-infrared to longer wavelengths and assuming that any excess is due to radiation from the secondary.

The eclipse depth method yielded a temperature of 350 K for the secondary. This method involves the fewest assumptions, so our expectation was that its results would be the most accurate, were it not for the fact that the solution for the secondary's spectrum also gave a solution for the primary's spectrum that we considered unlikely. The implication of this method was that the primary has a continuum beyond 5 μm that is much steeper than a blackbody curve for the star's temperature.

The second method, using the assumption that the primary star's spectrum can be extrapolated using a blackbody function, gave a temperature for the secondary of 650 K. In our paper we pointed out the apparent problem, and reported the temperature as 500 $\pm$ 150 K. New information from ground-based infrared observations in the second half of the eclipse plus IRAS spacecraft observations resolve this problem and yield a value of 475 $\pm$ 50 K (see below).

An important result from the ingress-phase infrared study regarding the physical nature of the secondary is the conclusion that the secondary object has a very low observed bolometric luminosity for its mass. If the secondary has a uniform temperature of 500 K and a distance of 1200 pc, its total observed flux is only 100 $L_\odot$; inclusion of a possible hot core emitting in the ultraviolet (Parthasarathy and Lambert 1983; Bohme, Ferluga, and Hack 1984) brings this up to only a few hundred $L_\odot$, a factor of 100 less than that expected for a mass of 16 $M_\odot$, which is the secondary's mass if the primary's mass is 20 $M_\odot$. [A much lower mass for the system has recently been proposed (Eggleton and Pringle 1985; Webbink, these proceedings)]. The term "observed" luminosity is used here to indicate the probability that a significant fraction of the radiation from an object embedded in a disk can escape along the polar directions, so the temperature of the rim of the disk may not characterize the total emission. Even so, it is very unlikely that 99% of the flux from the central object could be unobserved. Some possible explanations for the discrepancy between the mass and luminosity of this object are that the secondary's central mass is a black hole (Cameron 1971), or that the mass is split into two stars, a binary embedded in the disk (Lissauer and Backman 1984; Eggleton and Pringle 1985).

Another result from the infrared study comes from reasoning that the luminosity of the primary is capable of heating solid material in the side of the secondary facing it to a temperature of ~1100 K. This would indicate that the secondary must be completely opaque because a much lower temperature is measured for the side facing us during eclipse. The flux from the primary illuminating the secondary is independent of the actual luminosity of the primary because the luminosity scales with the system dimensions in a "standard" geometry in which the secondary does not have a central aperture and its moving edge can be used to measure the diameter of the primary (cf. Wilson 1971).

Infrared photometry of the system was continued by the UH/KPNO group through the rest of the eclipse and into the present post-eclipse phase. Figure 2 is a comparison of the shapes of the full light-curve at 2.2 μm with the combined visual record. The near-infrared and some of the 10 μm observations after mid-eclipse were performed by Dick Joyce and Ron Probst of KPNO as part of a standard star and red-variable photometry program in collaboration with Mike Merrill and Fred Gillett. Again, the normalization used here is the full-eclipse mean at the two wavelengths rather than an out-of-eclipse baseline comparison. Infrared observations were not made during the time when ϵ Aur was in conjunction with the sun. It is clear that the near infrared eclipse follows the visual curve very closely. The last data point is from 1984 December 5.

Figure 3 is the 10.1- and 20-μm data for the complete eclipse plotted for comparison with the 2.2 μm data. The complete eclipse bears out the conclusions made on the basis of the ingress observations. The eclipse was symmetric to first order about its mid-point in the infrared as well as at visual wavelengths.

Table 1 gives the dependence of eclipse depth on wavelength for all the infrared bands using all the available data; the baseline magnitudes are defined using a mean of pre- and post-eclipse observations. On the basis of our ingress measurements, we tentatively concluded that flux from the secondary had been detected at 5 μm at a $\sim 2\sigma$ level. The complete eclipse information now shows evidence of the secondary's presence only at 10 and 20 μm. The mean near-infrared eclipse depth is 0.68 mags, a little shallower than the result from the ingress observations.

The IRAS satellite (Neugebauer *et al.* 1984) made two special (non-survey) observations of ϵ Aur during full eclipse. Table 2 and Figure 4 show the flux from the secondary in the mid- and far-infrared, combining the ground-based and spacecraft results. The IRAS fluxes have been color-corrected. The color temperature of the secondary object from 10 to 60 μm is 475 $\pm$ 50 K, close to the results from the ground-based observations alone. The significance of the IRAS data is the extension of the single temperature and low luminosity of the secondary to a wavelength of 60 μm (Backman and Gillett 1985).

The extrapolation of the primary's spectrum beyond 10 μm in Table 2 makes use of a $F_\nu \sim \nu^2$ slope, slightly steeper than a blackbody curve. This model for the primary and a better determination of the out-of-eclipse baseline causes the temperatures estimated for the ϵ Aur secondary by using the two methods described above to approximately converge.

Finally, the combined ground-based and IRAS infrared photometry gives a size for the 475 K secondary of $\sim 9 \times 10^{-16}$ sr. The solid angle subtended by the secondary implies an aspect ratio (length^2 /area) of ~ 2, a surprising result. This result is independent of the distance to the system, again because of the connection between distance and the orbit scale in a "standard" geometry. The small aspect ratio could be due to agitation of the disk material by the embedded object(s), e.g., a rapidly revolving, close, massive binary.

We now know the wavelength region in which the secondary is most easily detected directly. That fact will allow our calculations of the size of the secondary and the amount of heating it receives from the primary to be easily checked as the secondary continues in its 27-year orbit. Infrared observations of ϵ Aur will be continued to further constrain our picture of this unusual system.

References

Backman, D. E., Becklin, E. E., Cruikshank, D .P., Joyce, R. R., Simon, Theodore, and Tokunaga, A. 1984, *Ap. J.*, **284**, 799.

Backman, D. E., and Gillett, F. C. 1985, submitted to *Ap. J.*

Becklin, E. E., Matthews, K., Neugebauer, G., and Willner, S. P. 1978, *Ap. J.*, **220**, 831.

Boehm, C., Ferluga, S., and Hack, M. 1984, *Astr. Ap.*, **130**, 419.

Cameron, A. G. W. 1971, *Nature*, **229**, 178.

Eggleton, P. P., and Pringle, J. E. 1985, *Ap. J.*, **288**, 275.

Hopkins, J., and Stencel, R. 1983, *Epsilon Aurigae Campaign Newsletter* # 9.

Lissauer, J. J., and Backman, D. E. 1984, *Ap. J. Lett.*, **286**, L39.

Neugebauer, G., *et al.* 1984, *Ap. J. Lett.*, **278**, L1.

Parthasarathy, M., and Lambert, D. L. 1983, *Pub. Astr. Soc. Pac.*, **95**, 1012.

Wilson, R. E. 1971, *Ap. J.*, **170**, 529.

TABLE 1

Infrared Eclipse Depth vs. Wavelength;
All data 1980-84

Band	λ (μm)	Mean Eclipse Depth (mag)
J	1.25	0.68 ± .01
H	1.65	0.68 ± .01
K	2.2	0.67 ± .01
L'	3.8	0.67 ± .01
M	4.8	0.68 ± .01
N	10.1	0.58 ± .02
Q	20	0.42 ± .06

TABLE 2

Infrared Flux During
1983 August-September (Full Eclipse)

λ (μm)	Observed Flux Corr. for A_λ [b] (Jy)	Extrapolated Primary (Jy)	Excess ≡ Secondary (Jy)
10.1[a]	9.1 ± .5	7.2 ± .3	1.9 ± .6
12	6.7 ± .3	5.1 ± .2	1.6 ± .4
20[a]	2.7 ± .15	1.8 ± .1	0.9 ± .2
25	2.0 ± .1	1.2 ± .05	0.8 ± .1
60	0.46 ± .03	0.20 ± .01	0.26 ± .03

[a]Ground-based

[b]Corresponding to A_V = 1.1 mag (Ake, these proceedings), scaled using the curve in Figure 1 of Becklin *et al*. 1978.

FIGURE 1

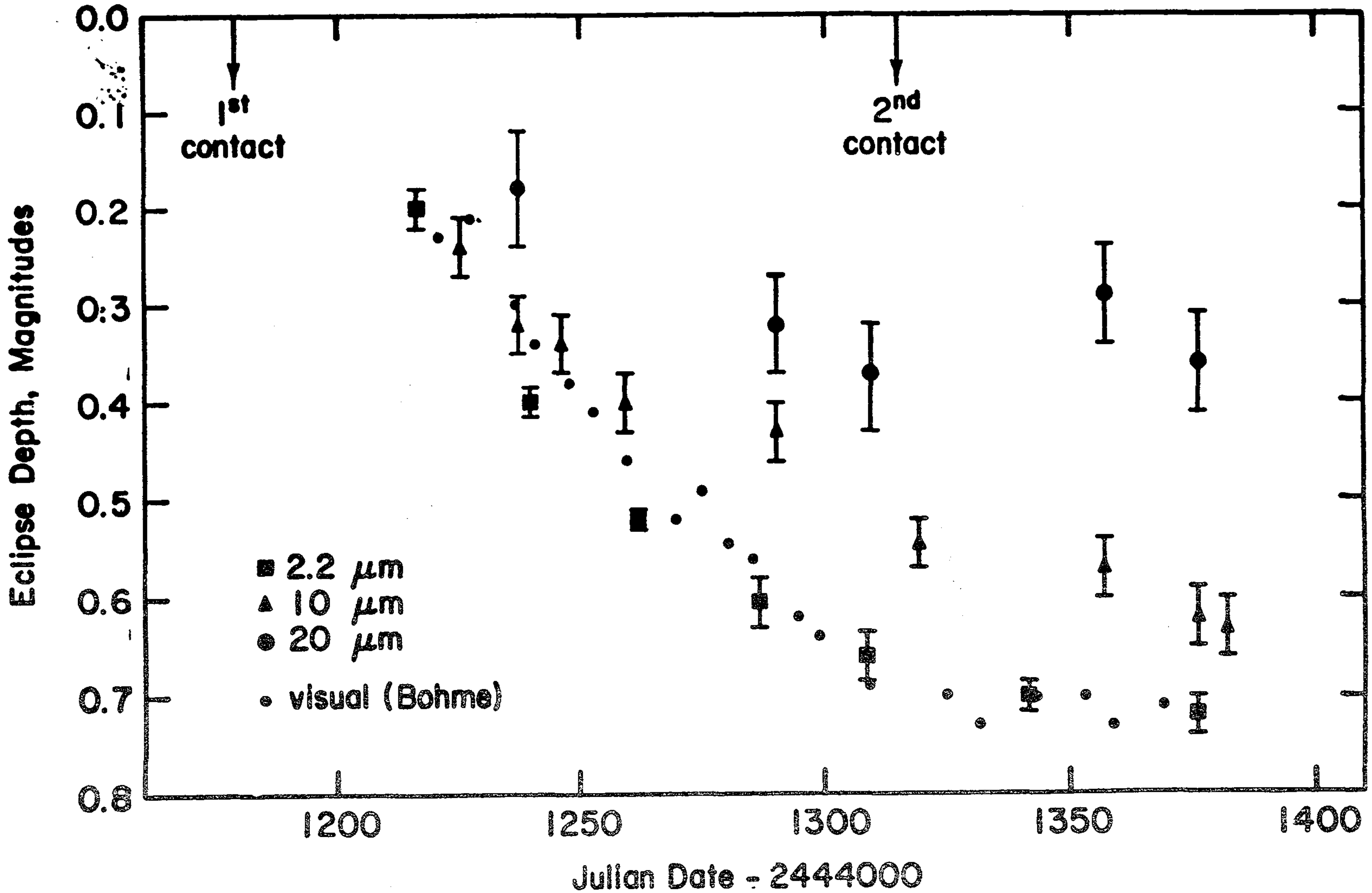
0.0
0.1
0.2
0.3
0.4
0.5
0.6
0.7
0.8
Eclipse Depth, Magnitudes
1st contact
2nd contact
2.2 µm
10 µm
20 µm
visual (Bohme)
1200
1250
1300
1350
1400
Julian Date - 2444000

FIGURE 2

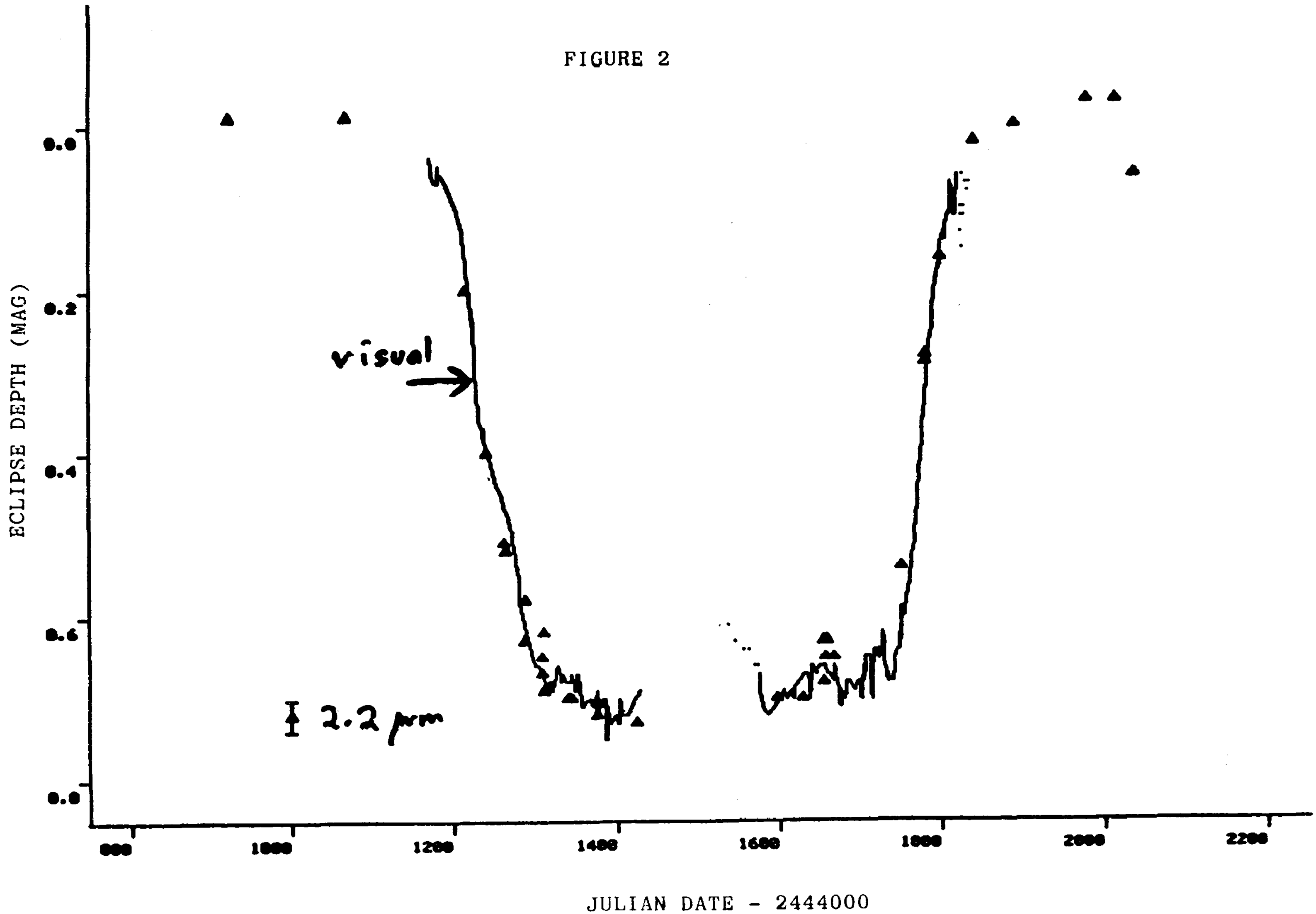

ECLIPSE DEPTH (MAG)
0.0
0.2
0.4
0.6
0.8
visual
2.2 µm
800
1000
1200
1400
1600
1800
2000
2200
JULIAN DATE - 2444000

FIGURE 3

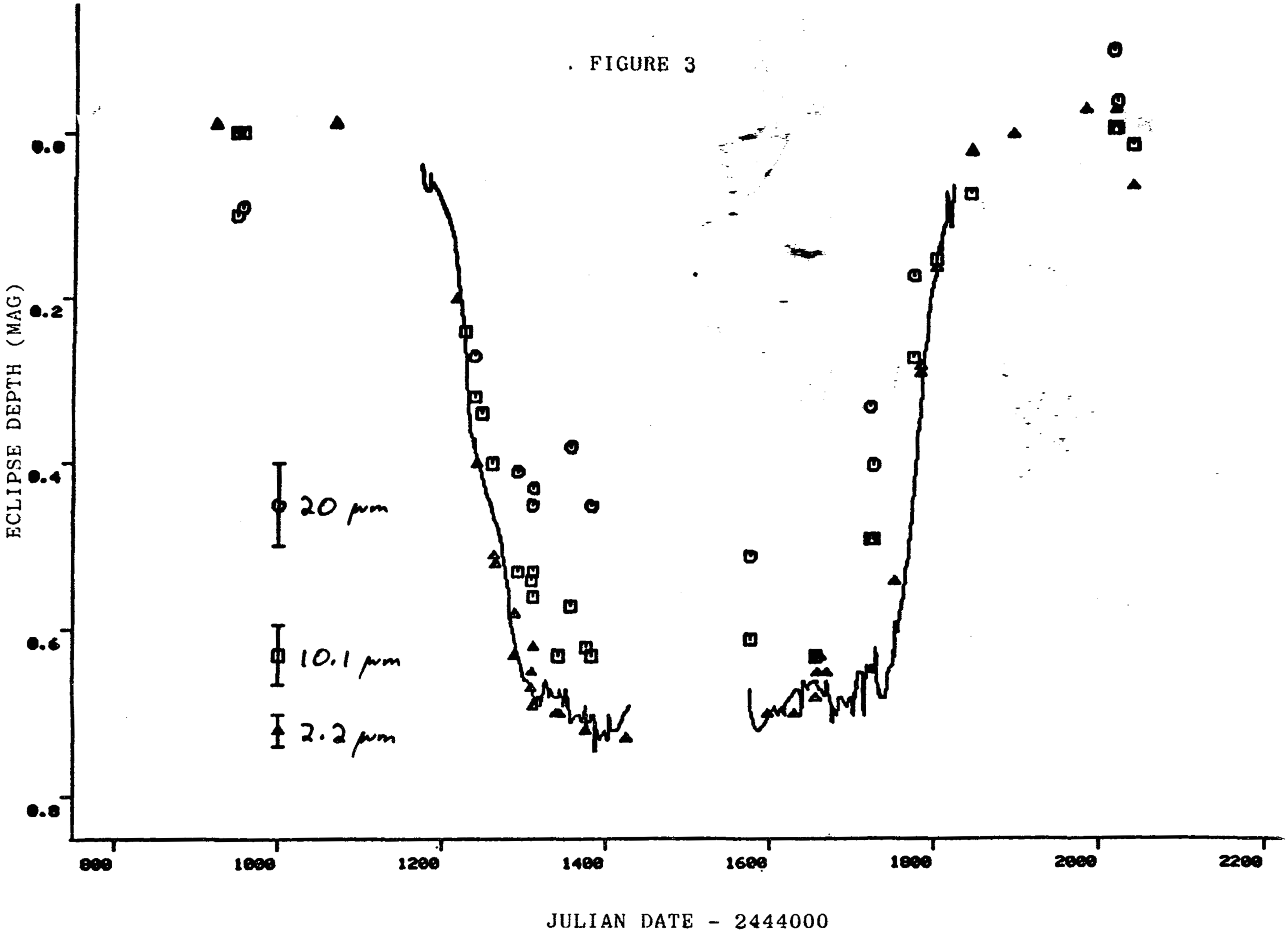
ECLIPSE DEPTH (MAG)
0.0
0.2
0.4
0.6
0.8
20 μm
10.1 μm
2.2 μm
800
1000
1200
1400
1600
1800
2000
2200
JULIAN DATE - 2444000

FIGURE 4

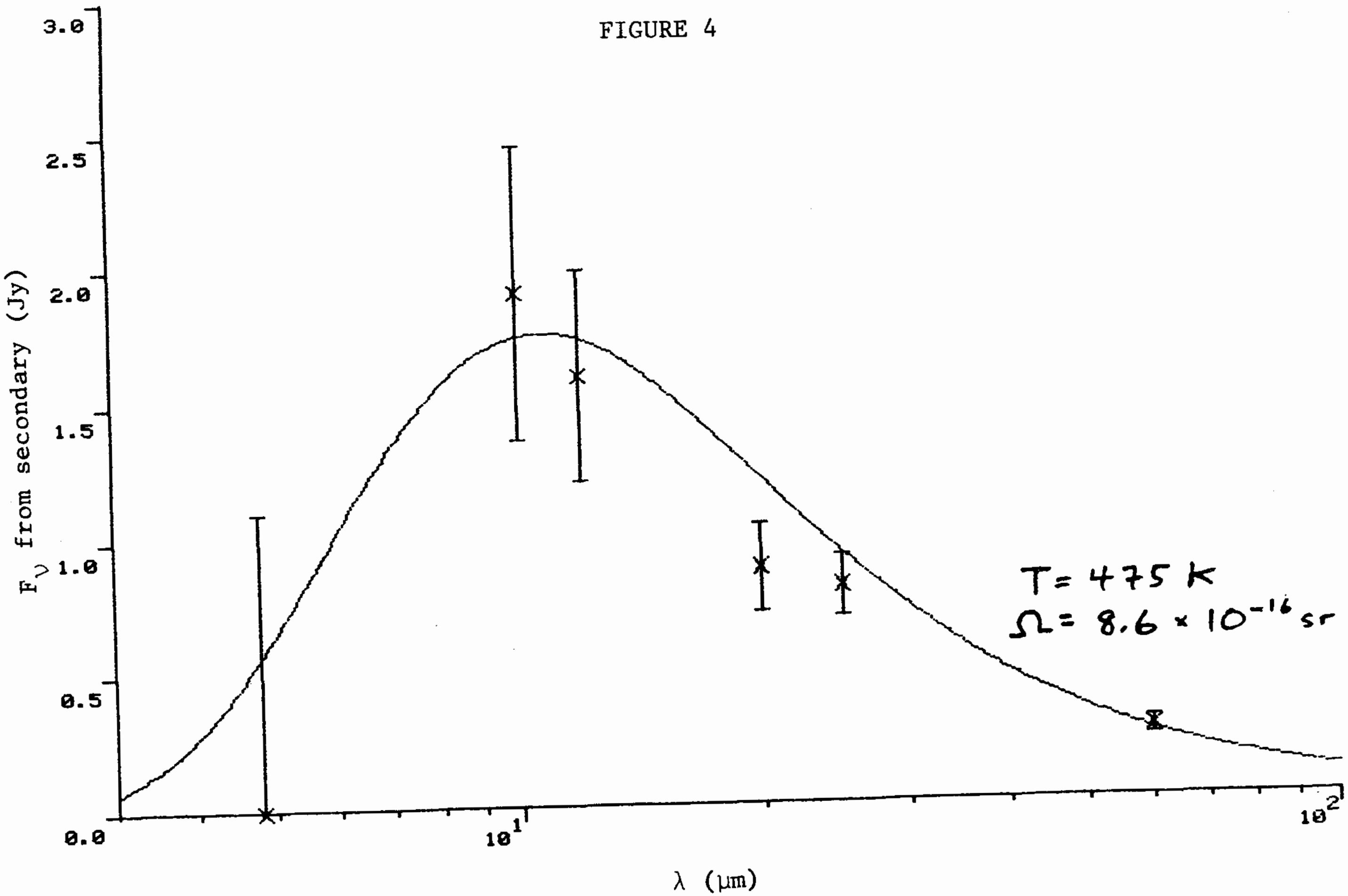
3.0
2.5
2.0
1.5
1.0
0.5
0.0
F_ν from secondary (Jy)
10^1
10^2
λ (μm)
T = 475 K
Ω = 8.6 × 10^-16 sr